

New explanation of the physics of tunnel effect processes

Viktar Yatskevich¹

¹Viktar Yatskevich, Ph.D,
CEO «Ltd.HYACINTH»,
Aurora, CO, USA
ltd.hyacinth@gmail.com

Abstract

The tunnel effect, commonly defined as the phenomenon in which a microparticle overcomes a potential barrier that exceeds its total energy, is often cited in quantum mechanics. However, this effect does not actually occur in its described form in nature, and the quantum mechanical interpretation of tunneling does not accurately represent the real physical processes involved, but rather provides a mathematical model. The true physical mechanism of the tunnel effect remains unidentified.

An analysis of the tunnel effect reveals that its manifestation creates a "paradox" in classical physics. Explanations based on the Heisenberg uncertainty principle and the wave nature of particles fail to offer a comprehensive understanding of the actual physical process.

This study proposes a new explanation of the tunneling phenomenon based on the principles of classical physics and electrodynamics. It is shown that the overcoming of the Coulomb barrier by low-energy microparticles occurs exclusively due to brief localized decreases in potential within the Coulomb barrier, allowing certain charged microparticles to penetrate.

The formation mechanism of these short-lived localized regions, which manifest as volume channels with lower potential within the Coulomb barrier, is examined. It is established that the creation of these channels is linked to the properties of atomic nuclei and their associated electric fields. This facilitates the suprabarrier penetration of the Coulomb barrier by individual low-energy microparticles, which pass through these channels while experiencing a reduction in their total energy.

This explanation resolves the "paradox" of the tunneling effect, eliminating the contradiction with classical physics laws. Moreover, the derived estimates of the tunneling process parameters are in qualitative agreement with the results obtained from quantum-mechanical models. The proposed framework aligns with nuclear physics findings, is supported by experimental evidence, and provides a new mechanism for controlling the tunneling effect in various energy-related applications.

Keywords: tunnel effect, potential barrier, Coulomb barrier, classical physics, quantum mechanical process, uncertainty principle, local area, microparticle, energy.

Introduction

Tunnel Effect and its Significance.

The tunnel effect is fundamental to various processes in atomic and molecular physics, nuclear physics, solid-state physics, chemistry, and other scientific fields. This phenomenon of quantum mechanics refers to the ability of an elementary particle to penetrate a potential barrier that is formed by the force field of other particles. The significance of the tunnel effect lies in its ability to allow charged particles, such as electrons or protons, to traverse a potential barrier whose height exceeds the total energy of these particles [1, 2].

In modern physics, the tunneling effect is considered a quantum mechanical phenomenon that primarily occurs within the microscopic realm. According to this framework, when the energy of a microparticle is insufficient to surmount a potential barrier, there exists a nonzero probability that the particle will appear in the region behind the Coulomb barrier without expending energy [3, 4].

Examples of the Tunnel Effect.

The tunneling effect accounts for a variety of experimentally observed phenomena, such as nuclear reactions in fusion, α - and β -decay, electron capture, and cold electron emission from metals. It also explains chemical processes, including ammonia inversion and formaldehyde polymerization at helium temperatures. Additionally, the tunneling effect has significant applications in electronics, including tunneling diodes, resonant tunneling diodes, double-layer tunneling transistors (DELTT), and single-electron transistors. These examples underscore the experimentally confirmed and critical role of the tunneling effect in numerous fields of both physics and engineering [5, 6, 7].

Current Understanding of the Physical Processes of the Tunnel Effect.

Given the tunnel effect's relevance to numerous discovered phenomena and its widespread use in engineering, understanding the underlying physical processes is crucial from both scientific and practical perspectives. The properties of the tunnel effect are governed by the Coulomb barrier, which is created by the electric fields of charged particles and their interactions with other charged entities.

Formation of the Coulomb Barrier.

(i) The formation of the Coulomb barrier is grounded in the principles of classical physics, particularly in the concept of electric fields created by point charges [8, 9, 10]. Electric charge is a fundamental property of matter that determines how the electric field affects other charged particles. Protons are positively charged (+Q), electrons are negatively charged (-Q), and neutrons are electrically neutral. The electric field (**E**) generated by a point charge **Q** dictates the strength of the electric field at a given position, defined by the position vector **r**.

$$\mathbf{E} = \frac{Q}{4 \cdot \pi \cdot \epsilon} \cdot \frac{\mathbf{r}}{|\mathbf{r}|^3} \quad (1)$$

where: **E** - is the field strength, **r** - is the vector drawn from the location of the charge + **Q** to the observation point, **|r|** - is the modulus of the vector **r**.

The image of the electric field strength lines **E** of a point charge +**Q** is shown in **Figure 1**.

The Coulomb field acts on a material body carrying a charge q , exerting a force of electric origin. The magnitude of this force is equal to the product of the charge's magnitude and the electric field strength at the location of the charge. The force \mathbf{F} acting on a point charge q due to the electric field \mathbf{E} is given by:

$$\mathbf{F} = q \cdot \mathbf{E} \quad (2)$$

where: \mathbf{F} - is the force acting on the point charge q from the side of the electric field \mathbf{E}
or:

$$\mathbf{F} = - \frac{Q \cdot q}{4 \cdot \pi \cdot \epsilon} \cdot \frac{r}{|r|^3} \quad (3)$$

The electrostatic force between charges Q and q can be understood as the interaction between charge q and the electric field generated by charge Q , and vice versa. The force \mathbf{F} experienced by charge q is the product of the charge q and the electric field \mathbf{E} at the position of charge q , denoted by the vector \mathbf{r} :

$$\mathbf{F}(\mathbf{r}) = q \cdot \mathbf{E}(\mathbf{r}) \quad (4)$$

(ii) The electric field at a point due to a system of point charges is the vector sum of the electric fields produced by the individual charges at that point. This field is determined by the principle of superposition, where the strengths of the fields from all charges are added vectorially (**Figure 2**)

The convergence of two point charges with identical magnitudes, $+Q$, results in the formation of a non-uniform electrostatic field. As the charges approach one another, the strength of the electrostatic field increases (**Figure 3**).

In the general case, the electric field \mathbf{E} , due to a system of charges, can be expressed as:

$$\mathbf{E} = \mathbf{E}_1 + \mathbf{E}_2 + \dots + \mathbf{E}_N = \frac{1}{4\pi\epsilon} \sum_{i=1}^N \mathbf{g}_i \cdot \frac{\mathbf{r}_i}{|r|^3} \quad (5)$$

where: \mathbf{E}_i - is the electric field strength created by charge g_i at a point with radius-vector \mathbf{r}_i , drawn from charge g_i , \mathbf{r}_i - is the distance between the charge and the point of space in which the field strength \mathbf{E} is calculated. In the case of a continuously distributed charge system, the electric field strength is determined by integrating over the charge distribution:

$$\mathbf{E} = \frac{1}{4\pi\epsilon} \int dq \mathbf{e}/r^2 \quad (6)$$

where: \mathbf{E} is a vector field that varies with position in space, and the integration is performed over the charge distribution to obtain the resultant electric field.

Coulomb barrier formation.

The Coulomb barrier is formed by a single charged entity, such as the nucleus of a hydrogen atom, or by a system of identically charged microparticles [2, 3, 11].

The Coulomb barrier of the nucleus is defined as the energy barrier that must be overcome by a positively charged particle to penetrate the nucleus. This concept is crucial for understanding processes such as nuclear fusion, where charged particles must surmount this barrier to interact with the nucleus.

When a charged microparticle approaches the Coulomb barrier, it experiences a repulsive force according to Coulomb's law. However, at very small distances on the order of **1 femtometer (fm = 10⁻¹⁵ m)** - the nuclear forces between the particles become stronger than the Coulomb forces and result in mutual attraction. As a result, the total interaction potential between the microparticles as a function of distance exhibits a maximum, corresponding to the top of the Coulomb barrier. At this point, two regions of space (denoted as regions 1 and 2) are separated by the potential barrier. The height of this barrier defines the minimum energy required for the microparticles to overcome the Coulomb barrier (**Figure 4**).

At large distances, Coulomb forces result in repulsion (region 2), whereas at small distances (region 1), nuclear forces dominate, leading to attraction. The magnitude of the potential barrier **U_{max}** is directly proportional to the charges of the interacting nuclei. For a strong nuclear interaction to occur and bind the nuclei together, they must attain sufficiently high velocities to overcome the Coulomb barrier (region 2) and enter the nuclear attraction region (region 1). For instance, two protons must overcome a Coulomb barrier with a height of approximately **1.1 MeV**, which corresponds to a temperature of nearly **1.3·10⁹ °C**, allowing them to approach distances on the order of **10⁻¹⁴ meters**.

The Coulomb barrier of a nucleus is characterized by its height **U** and width **a**, which depend on the energy of the interacting particles and are determined by the entry and exit points of the barrier. The potential energy of Coulomb repulsion for identically charged particles outside the nuclear force region is given by the equation:

$$U(\mathbf{R}) = Z_1 \cdot Z_2 / \mathbf{R}, \quad \mathbf{R} > r_0 \quad (7)$$

where: **Z₁ and Z₂** are the charge numbers of particles (**Z_i = Z · e**, **Z** is the atomic number), **R** - is the distance between particles, **r₀** is the radius of action of nuclear forces.

The height of the Coulomb barrier of the nucleus **U** corresponds to the electrostatic energy of interacting particles at a distance approximately equal to the sum of their nuclear radii:

$$U = 1,44 \cdot Z_1 \cdot Z_2 / R, \quad (8)$$

where: **Z₁ and Z₂** are charge numbers of particles, **U** - in MeV, **R** - in fermi (**1f = 10⁻¹⁵ m**).

Explanations of the physical processes of the tunnel effect at the present time.

(a) Classical physics. According to classical mechanics, the tunneling of particles through a potential barrier is considered impossible [2,3].

The laws of classical mechanics state that any material body, such as an elementary particle (e.g., an electron or a proton), with total energy **E = p²/2m + U(x,y,z)** can overcome a potential barrier of height **U₀** only if their energy **E** exceeds the height of the barrier, i.e. **E > U₀**. If the total energy is lower than the barrier height (**U₀ > E**) the particle cannot surpass the barrier and will instead be reflected from it, in accordance with the principle of energy conservation (**Figure 5**).

This principle also applies when a particle is within a potential barrier and has total energy **E** lower than the barrier height, i.e., **U₀ > E**. In classical mechanics, a particle can only exist in spatial regions where its potential energy **U** does not exceed its total energy. Tunneling beyond the barrier

would require the particle to possess negative kinetic energy, which contradicts classical physics, since momentum $\mathbf{p} = m\mathbf{V}$ must always be a real quantity.

Therefore, if two spatial regions are separated by a potential barrier, only classical over-barrier penetration of a charged particle is possible. The transmission of a charged particle through a barrier when its total energy \mathbf{E} , is lower than the barrier height \mathbf{U}_0 is fundamentally impossible within the framework of classical mechanics.

(b) Quantum mechanical description of the tunneling effect.

In modern physics, the tunneling effect is considered a purely quantum mechanical phenomenon, providing direct evidence of the wave-particle duality of elementary particles.

The physics of quantum tunneling is fundamentally based on the Heisenberg uncertainty principle and the wave-like nature of particles [2, 3, 4].

- Confining a microparticle within a narrow region of the barrier increases the uncertainty in its momentum, thereby increasing the probability of its transmission through the potential barrier due to energy redistribution.
- The particle exhibits wave-like properties, and its wave function is never entirely localized within a single region of the barrier. As a result, a portion of the wave function extends beyond the barrier, allowing the particle to tunnel through it (**Figure 6**).

Explanation Based on the Heisenberg Uncertainty Principle.

(a) The tunneling effect can be understood in terms of the Heisenberg uncertainty principle, which states that the position and momentum of a particle cannot both be precisely determined simultaneously: $\Delta\mathbf{x}\cdot\Delta\mathbf{p} \geq \hbar$, where $\Delta\mathbf{x}$ represents the uncertainty in the particle's position, and $\Delta\mathbf{p}$ represents the uncertainty in its momentum. This relation implies that localizing a quantum particle within a confined spatial region (i.e., decreasing $\Delta\mathbf{x}$) leads to a greater uncertainty in its momentum ($\Delta\mathbf{p}$). If a particle encounters a potential barrier of width \mathbf{a} , its positional uncertainty is approximately $\Delta\mathbf{x} \approx \mathbf{a}$. Consequently, the uncertainty in its momentum satisfies: $\Delta \mathbf{p} > \hbar/\mathbf{a}$ which can be large enough that the total energy of the particle \mathbf{E} exceeds the barrier height \mathbf{U}_0 .

As a result, even if the classical energy of the particle is less than \mathbf{U}_0 , quantum mechanics allows the particle to penetrate the barrier with a certain probability. This probability increases as the particle's mass decreases, the barrier width \mathbf{a} decreases, or the energy deficit ($\mathbf{U}_0 - \mathbf{E}_0$) decreases. Importantly, while the probability of penetration depends on these factors, the average energy of the transmitted particle remains unchanged. This approach provides an explanation of the tunneling effect based on the Heisenberg uncertainty principle.

(b) Explanation Based on the Schrödinger Equation.

The tunneling effect can also be understood by solving the time-independent Schrödinger equation:

$$\frac{d^2\psi}{dx^2} + \frac{2m}{\hbar^2} (E - U)\psi = 0, \quad (9)$$

where: $\psi(\mathbf{x})$ is the wavefunction of the particle and $\mathbf{U}(\mathbf{x})$ represents a stationary potential barrier.

In most cases, for simplification, this equation is analyzed in a one-dimensional scenario with a time-independent potential barrier. The solution reveals that the wavefunction does not vanish inside the

barrier but instead exhibits an exponential decay, leading to a finite probability of transmission even when $E < U_0$. This quantum mechanical behavior fundamentally distinguishes tunneling from classical motion. The solution of equation (1) has an oscillatory character for the regions before barrier 1 and after barrier 3:

$$\begin{aligned}\Psi_1(x) &= A \exp(i k_1 x) + B \exp(-i k_1 x) \\ \Psi_3(x) &= a \exp(i k_1 x) + b \exp(-i k_1 x),\end{aligned}\quad (10)$$

where: $k_1 = \pm 1/\hbar \sqrt{2mE}$, A, a - is the amplitude of the incident wave, $A = 1, B, b$ - is the amplitude of the reflected wave, $B = 0$.

For region 2 inside the barrier, the solution is obtained in exponential form:

$$\Psi_2(x) = \alpha \exp(ik_2 x) + \beta \exp(-ik_2 x), \quad (11)$$

where: $k_2 = \pm 1/\hbar \sqrt{2m(U - E)}$, $\alpha \ll \beta$

The solution of the equation allows us to determine the wave function $\psi(x)$ and the probabilities of particle detection $\psi^2(x)$ when passing through the potential barrier over the entire coordinate interval x in different regions **1, 2** and **3** (Figures 6, 7).

The solution leads to the following qualitative estimates:

- there is a probability that the particle will be reflected from the barrier and move in the opposite direction if $E > U_0$;
- there is a probability that the particle will be outside the barrier in the region $x > a$, where a is the barrier width, i.e., it will pass through the barrier if $E < U_0$.

A particle can tunnel through a potential barrier with a certain probability, given by $|\psi(x)|^2$ for $x > a$, and propagate to the right in the region beyond the barrier. If the barrier has a finite width a and is sufficiently narrow such that $a < \lambda_D$, then the total probability of the particle being either transmitted through or reflected from the barrier must sum to one. Consequently, the amplitude of the wave reflected from the barrier is smaller than that of the incident wave (Figure 7).

For a one-dimensional potential barrier, the primary factor determining the probability of transmission is the barrier transparency coefficient, denoted as D . This coefficient is defined as the ratio of the flux of transmitted particles to the flux of incident particles on the barrier. The solution of the Schrödinger equation provides an expression for D in terms of wave amplitudes:

$$D = |A_3|^2 / |A_1|^2 \quad (12)$$

or after substituting explicit values:

$$D = D_0 \exp(-2/\hbar \cdot \sqrt{2m(U - E)} \cdot a) \quad (13)$$

where: U is the height of the potential barrier, E is the energy of the particle, a is the width of the barrier, D_0 is a constant approximately equal to 1, m is the rest mass of particles.

According to this relation, the characteristic thickness of the potential barrier is determined by:

$$a \approx \frac{1}{2/\hbar \sqrt{2m(U - E)}} \quad (14)$$

From expressions above, the following conclusions can be drawn:

- The probability of a particle tunneling through the barrier decreases as its mass m and the barrier width a increase.
- The probability of transmission increases as the potential barrier height U decreases for a given energy E .
- The barrier permeability coefficient is much more sensitive to changes in the width of the barrier than to changes in its height.
- If the barrier is not relatively narrow, the probability of tunneling becomes exponentially small.

In real physical systems, potential barriers are rarely perfectly rectangular. The specific shape of the barrier affects the quantitative tunneling probability but does not alter the qualitative nature of the tunneling effect. The formula above can be generalized to barriers of arbitrary shape by dividing the interval $0 \leq x \leq a$ into sufficiently small segments Δx_i , within which the potential energy U_i can be approximated as constant (**Figure 8**).

The probability W_i that a particle will pass an elementary site is obtained by replacing U_0 by U_i and a by Δx_i :

$$W_i = \exp \left[-\frac{2}{\hbar} \sqrt{2m(U_i - E)} \cdot \Delta x_i \right] \quad (15)$$

Due to the independence of the individual elementary events, the probability of passing through the entire barrier of width a is equal to their product:

$$W(L) = \prod_i W_i = \exp \left[-\frac{2}{\hbar} \sum_i \sqrt{2m(U_i - E)} \cdot \Delta x_i \right] \quad (16)$$

In the general case (16) goes to the integral entry:

$$W(L) = \exp \left[-\frac{2}{\hbar} \int_0^L \sqrt{2m(U(x) - E)} dx \right] \quad (17)$$

and the thickness of a potential barrier of arbitrary shape, at which the tunneling effect acts is determined by the induction:

$$a \approx \frac{1}{2/\hbar \int \sqrt{2m(U-E)} dx} \quad (18)$$

Consideration of more complicated variants of determining the parameters of the tunnel effect shows that their results do not qualitatively differ from those mentioned above [3,12,13,14].

Analysis of Quantum Mechanical Explanations of the Tunneling Effect.

a) The existence of the tunneling effect, which allows a particle to penetrate a potential barrier even when its energy is lower than the barrier height, can only be explained within the framework of quantum mechanics.

A fundamental quantum mechanical explanation of the tunneling effect is based on the Heisenberg uncertainty principle. From this perspective, as the particle passes through the barrier, its energy E appears to increase by the amount:

$$\frac{\Delta p^2}{2m} = \Delta E = U - E \quad (19)$$

where: $\Delta p^2 = \hbar / 4 \cdot a^2$ represents the minimum momentum dispersion of the particle.

However, it is important to note that the energy of the transmitted particle remains unchanged, meaning that no net energy is expended in the tunneling process.

Key considerations regarding this explanation include:

- The uncertainty relation $\Delta x \cdot \Delta p \geq \hbar$ was originally formulated to define the limits of precision in measuring the position and momentum of quantum particles. While the uncertainty principle is essential in the statistical interpretation of quantum experiments, it does not directly explain the physical mechanism of tunneling.
- Planck's relation $E = \hbar \cdot \omega$, where $\omega = 2 \cdot \pi \cdot \nu$ is the circular frequency of radiation, applies to quantized electromagnetic transitions at the atomic and nuclear levels and does not directly relate to the tunneling effect.
- Explaining tunneling solely based on the uncertainty principle provides a mathematical model of the effect but does not fully describe the physical process of quantum particle transmission through a barrier.

(b) A more detailed quantum mechanical interpretation of tunneling relies on the wave properties of microparticles, specifically the de Broglie wave function. In this view, the amplitude of the de Broglie wave is treated as a probabilistic characteristic. The probability of locating a particle in a particular region of space is given by the square of the wave function amplitude, $|\psi(\mathbf{x})|^2$.

As a quantum particle encounters a potential barrier, its wave function exhibits exponential decay inside the classically forbidden region. However, the frequency and total energy of the wave remain constant. The probability of transmission through the barrier is determined by the square of the residual wave amplitude beyond the barrier.

Key points regarding this approach:

- The de Broglie wave provides a mathematical representation of the tunneling effect rather than a direct physical mechanism.
- The Schrödinger equation, which governs the evolution of the wave function $\psi(\mathbf{x})$, is used to determine the probability $|\psi(\mathbf{x})|^2$ of finding a particle in a given region. While this equation predicts tunneling behavior, it does not explicitly explain the physical process behind it.

Conclusions on the Tunneling Effect.

- Tunneling is impossible within classical mechanics because it contradicts fundamental classical principles, such as the conservation of energy in the classical sense.
- Experimental evidence confirms the existence of tunneling in nature, with particles possessing insufficient energy still having a probability of passing through potential barriers. This phenomenon, often considered paradoxical from a classical perspective, has been experimentally observed in fields such as quantum transport, nuclear fusion, and superconductivity.
- Quantum mechanical models based on the uncertainty principle and wave functions provide accurate estimates of tunneling parameters but do not fully describe the underlying physical mechanism.
- The tunneling effect is best understood as a consequence of the wave nature of matter, rather than as a direct result of energy fluctuations or measurement uncertainty.
- The precise physical mechanism of tunneling remains an open question in quantum mechanics. While current models predict the statistical behavior of particles with great accuracy, the exact nature of the transition process through the barrier is still not fully understood.

Results.

(i) Objective of the Study

The primary aim of this study was to investigate the physical mechanisms underlying the tunneling effect, as the conventional quantum mechanical description does not provide a direct understanding of the real physical process involved. The key result of the study is an alternative explanation of the tunneling effect based on classical mechanics, electrostatics, and electrodynamics. The study suggests that tunneling occurs due to localized reductions in potential within the Coulomb barrier, enabling individual microparticles to traverse the barrier in these specific regions.

The formation of such low-potential regions is attributed to the intrinsic properties of charges that generate the Coulomb field. This explanation resolves the so-called “paradox” of the tunneling effect by eliminating its contradiction with classical physics. Moreover, the estimated parameters of the tunneling process derived from this model qualitatively align with the results of quantum mechanical calculation.

(ii) Mechanism of Microparticle Barrier Penetration

Microparticles can overcome a potential barrier formed by the Coulomb field through the following mechanisms:

- Above-barrier transmission: when the total energy \mathbf{E} of a microparticle exceeds the height of the potential barrier \mathbf{U}_0 , the microparticle classically overcomes the barrier: $\mathbf{E} > \mathbf{U}_0$;
- Suprabarrier transmission via localized potential reduction: when the potential barrier momentarily decreases in a localized region, the effective barrier height $\mathbf{U}_{\min}(\mathbf{x}, \mathbf{y}, \mathbf{z}, \mathbf{t})$ is reduced, allowing the microparticle to pass through if: $\mathbf{E} > \mathbf{U}_{\min}$.

This mechanism is identified as a “virtual tunneling effect”, where low-energy microparticles pass through the Coulomb barrier when a localized temporary potential reduction occurs.

The probability of this effect depends on:

- The characteristics of the potential field responsible for the fluctuating barrier.
- The coincidence of a microparticle’s approach with the moment of barrier reduction.
- The energy, mass, spatial orientation, and concentration of the microparticles.

Key Conclusion.

The tunneling effect can be interpreted exclusively as a suprabarrier transmission mechanism, where microparticles pass through localized regions of reduced potential rather than violating classical energy conservation. Notably, the study suggests that the total energy of microparticles decreases as they pass through the barrier, a phenomenon previously overlooked because instantaneous potential reductions within the barrier were not accounted for.

Reevaluation of the Conventional Quantum Mechanical Explanation.

The traditional quantum mechanical tunneling model assumes that a microparticle can penetrate a potential barrier that exceeds its total energy. However, this study argues that such a process does not actually occur in nature. Instead, the misunderstanding arises from the oversimplification of the real spatial and temporal structure of the potential barrier.

Errors in the conventional interpretation of tunneling include:

(i) Misconception of barrier properties:

- The potential barrier $U(\mathbf{x},\mathbf{y},\mathbf{z},\mathbf{t})$ is assumed to be static, ignoring spatial and temporal variations that create localized potential reductions.

Idealization of the Coulomb field:

- The Coulomb potential is treated as a time-independent electric field generated by point charges, overlooking the complex field interactions that may form radial channels of lower potential.
- For instance, the electric field of a proton or hydrogen isotope nucleus is often represented as that of an idealized point charge $+e$, leading to oversimplified barrier models.

(ii) Failure to account for potential barrier fluctuations:

- The height of the potential barrier depends on charge interactions and interparticle distance.
- However, conventional models do not consider localized reductions that can create transient, low-potential pathways for particle transmission.

(iii) Incorrect application of quantum mechanics:

- The Heisenberg uncertainty principle and the Schrödinger equation are used to describe tunneling through a constant potential barrier U_0 , disregarding its dynamic nature.
- Quantum mechanics models the Coulomb barrier electrostatically, while simultaneously treating moving microparticles as both waves and particles, which does not provide a coherent understanding of the physical transmission process.

(iv) Incorrect assumption about kinetic energy conservation:

- It is erroneously believed that the kinetic energy E of a microparticle remains constant during tunneling. This contradicts the study's findings, which indicate that energy decreases as the microparticle crosses through localized regions of reduced potential.

The widespread idealization of the Coulomb barrier parameters and the assumption that microparticles retain their total energy while traversing a potential barrier represent a fundamental error in modern tunneling descriptions. This leads to an apparent contradiction with classical physics, although quantum mechanical models still provide mathematically valid solutions.

According to this study, tunneling occurs due to short-term reductions in the potential barrier within localized regions, enabling the transmission of low-energy microparticles. This approach aligns with the law of conservation of energy in classical physics while introducing a probabilistic aspect, as

a microparticle can only pass through if it arrives at the barrier precisely when the potential reduction occurs. This revised interpretation challenges the traditional view of tunneling and offers a new framework for understanding microparticle interactions in dynamic Coulomb fields. Indeed, a microparticle can overcome the potential barrier if the barrier level U in the local region is lower than the total energy E of the microparticle during its passage through the region (**Figure 1**).

Such “virtual tunnelling effect” does not contradict the law of conservation of energy in classical physics, and the possibility of microparticles getting into the local region of the barrier at the moment of a short-term decrease in the potential in this region has a probabilistic character.

It is important to note that during the transition through a potential barrier, the total energy of microparticles decreases by an amount equal to the potential energy of the barrier within the localized region during the barrier passage time. This relationship is expressed as:

$$E_2 = E_1 - U(\mathbf{x}, \mathbf{y}, \mathbf{z}, \mathbf{t}) \cdot \mathbf{a}, \quad (20)$$

where: E_1 is the total energy of the microparticle before passing the barrier,, E_2 is the total energy of the microparticle after passing the barrier,, $U(\mathbf{x}, \mathbf{y}, \mathbf{z}, \mathbf{t}) \cdot \mathbf{a}$ - represents the potential energy of the localized barrier region of width \mathbf{a} at the moment the microparticle moves through it.

This energy reduction mechanism has not been previously observed because traditional models do not account for the instantaneous decrease in barrier potential in localized regions as microparticles traverse them. The study emphasizes that this effect plays a fundamental role in understanding the real physical process underlying the tunneling effect. It is important to highlight that the possibility of suprabarrier tunneling due to “tunnel barrier oscillations” has been previously suggested in scientific literature.

These works propose that fluctuations in the barrier height can momentarily reduce the potential barrier, increasing the probability of a low-energy particle passing through the barrier at the instant of its oscillation minimum. A proposed cause of such barrier oscillations is the dynamic fluctuation of charge density, which forms the Coulomb field.

These fluctuations may arise from:

- Vibrations, oscillations, and rotations of atomic nuclei.
- Dynamic charge density changes in the crystal lattice.

However, previous studies did not quantify the parameters of barrier oscillations and their exact effect on microparticles, nor did they indicate more significant factors contributing to the localized decrease of the Coulomb barrier height [15, 16].

At present, the Coulomb barrier oscillation is associated with the elastic properties of nuclei and changes in the charge density in nuclei. This oscillation of the Coulomb field reduces the energy threshold level in some directions and time, but as will be shown below, this is not sufficient to explain the tunneling effect.

Result.

New Explanation of the Physical Processes Involved in the Tunneling Effect.

Different types of charge systems that generate the Coulomb field vary in how they create the volume profile of the potential barrier $U(\mathbf{x}, \mathbf{y}, \mathbf{z}, \mathbf{t})$ and in the type of tunneling particles involved (such as protons, electrons, etc.). However, the fundamental structure and interaction of elements during the tunneling effect can be generalized across different systems. Studies show that the physics underlying tunneling processes does not qualitatively differ between various systems.

As an example, we consider a specific variant of the tunneling effect in which positively charged particles – protons overcome the Coulomb barrier while penetrating the atomic nucleus. This variant holds the most significant practical importance.

A. Amplitude Diagram of Electric Field Directivity.

The electric fields of atomic nuclei form the foundation of the Coulomb field. The charge of an atomic nucleus creates an electric field \mathbf{E} in space, whose effect can be estimated using the amplitude directional diagram (**ADD**). The principle of formation **ADD** is similar to that of antenna directional diagrams [17,18].

The **ADD** represents the variation in the amplitude of electric field strength \mathbf{E} at equidistant points at a distance \mathbf{R} from the charge center or charge system, with angular coordinates θ_i and ϕ_i :

$$\mathbf{F}_{\text{add}} = \mathbf{E}_i(\mathbf{R}, \theta_i, \phi_i, t_i), \quad (21)$$

where: \mathbf{F}_{add} is the amplitude directivity diagram, \mathbf{E}_i is the amplitude of electric field strength at point \mathbf{i} , \mathbf{R}_i is the distance from the center of the charge, θ_i, ϕ_i are the angular coordinates of the observation point (elevation angle and azimuth), t_i is the time moment under consideration.

The **ADD** is a three-dimensional spatial surface that describes the Coulomb field's distribution at a given moment. The shape of the **ADD** depends on the magnitude and distribution of charges in the atomic nucleus, as well as on the presence of absorbing and shielding elements in the electric field. The **ADD** can be represented graphically and analyzed in different planes (**Figure 9**).

Due to the influence of electric fields from all protons in the space surrounding the nucleus, a bulk Coulomb barrier is formed, with its configuration described by the **ADD**. The **ADD** provides insights into the potential barrier height U as a function of direction and determines the Coulomb field's force on external charged particles. The **ADD** shape of the atomic nucleus's electric field, from its conventional center to the maximum barrier height, allows us to evaluate the likelihood of a charged particle penetrating the nucleus via supra-barrier transition.

B. Formation of the Coulomb barrier by atomic nuclei.

(i) The Atomic Nucleus as the Basis for the Coulomb Barrier

The atomic nucleus is the central part of the atom, where almost all its mass and positive electric charge are concentrated. Atomic nuclei consist of protons p and neutrons n , bound together by nuclear interactions. The range of nuclear forces is limited to approximately $\sim 10^{-15}$ m.

The nuclear forces acting between a proton and a neutron, as well as between two neutrons, are assumed to be identical. Both the proton and neutron have finite sizes and an internal structure composed of fundamental particles (**Figure 10**).

Most atomic nuclei are nearly spherical in shape. The size of a nucleus is characterized by its radius, which has a conditional meaning due to the blurred boundary of the nucleus. The radius can be approximated using the following formula:

$$R \approx 1.3 - 1,7 \cdot 10^{-15} A^{1/3} \text{ m}, \quad (22)$$

where: **A** is the number of nucleons (total number of protons and neutrons) in the nucleus.

Nuclei with a low number of nucleons have diameters on the order of 10^{-15} m. For example, the proton's radius is approximately $4.5616 \cdot 10^{-16}$ m, with a small fraction of its mass extending beyond this radius. Similarly, the neutron's radius is $4.5616 \cdot 10^{-16}$ m, while its outer limit is $4.3913 \cdot 10^{-16}$ m from the particle's center. Most chemical elements contain more neutrons than protons because, for structural stability, neutrons are required between the protons [11, 19].

Properties of Protons and Neutrons

Modern research reveals that protons and neutrons exhibit the following properties:

- The proton has a positive electric charge equal in magnitude to the elementary charge: $+e = +1,602\ 176\ 634 \cdot 10^{-19}$ C.
- The proton's electric field is similar to that of a point charge $+e$, but it exhibits variations due to proton motion, changes in surface charge density, and interactions with neutrons in the nucleus.
- The potential and electric field strength of a proton at a far-field point are given by:

$$\varphi(\mathbf{A}) = +e / 4\pi \epsilon_0 R, \quad \mathbf{E} = +e \mathbf{n} / 4\pi \epsilon_0 R^2 \quad (23)$$

where: $+e$ is the elementary electric charge, ϵ_0 is the electric constant, \mathbf{n} is a unit vector from the proton's center toward the observation point, and \mathbf{R} is the distance from the proton center to the observation point, where $\mathbf{R} > \mathbf{R}_p, \mathbf{n}$.

The neutron has a permanent magnetic field and an intrinsic electric field formed by distributed parallel symmetric ring electric charges of $+0.75e$ and $-0.75e$, with a mean radius r_e located at a distance s :

$$\begin{aligned} r_e &= 1,0626 \cdot h / m_0 \cdot c \\ s &= 0,85 \cdot L \cdot h / m_0 \cdot c \end{aligned} \quad (24)$$

The neutron's constant electric field resembles a dipole field, similar to that of two distributed parallel electric charges of equal magnitude but opposite signs. Since the neutron has a net charge of zero, its electric field is nearly imperceptible at larger distances due to charge cancellation. However, this field affects interactions with protons and other neutrons at distances comparable to the neutron's radius.

A significant property of the neutron is its low permeability to external electric fields. When placed in an external electric field \mathbf{E}_0 , the neutron's structure deforms, shifting the centers of its positive and negative charge distributions in opposite directions. This deformation transforms the neutron into a dipole aligned with the external field. The resulting bound charges on the neutron's surface create an internal field \mathbf{E}' that opposes \mathbf{E}_0 , leading to a reduced net field strength inside the neutron: $\mathbf{E} = \mathbf{E}_0 - \mathbf{E}' < \mathbf{E}_0$. Additionally, structural changes induce internal energy losses.

Consequently, the external electric field strength decreases by a factor of approximately 10^{-20} dB in the neutron's shadow region. Thus, the main properties of nucleons as part of atomic nuclei are the charge and magnetic moment of the proton, the magnetic moment of the neutron, the neutron's neutrality (zero net charge), and the neutron's ability to attenuate an external electric field [19,20,21,22].

(ii) Peculiarities of Coulomb Field Formation by a Proton (Hydrogen Atom Nucleus)

The electric fields of protons are the main factor determining the effect of the atomic nucleus on the surrounding space. In most known cases, when considering the tunneling effect, the proton is represented as a charged ball with radius $R \approx 4.5616 \times 10^{-16}$ m with charge +e uniformly distributed over the surface. It is assumed that the force lines of the electric field of the proton are directed along the extension of its radii and distributed similarly to the force lines of the point charge +e. Indeed, the electric field E of the proton propagates into the surrounding space like the lines of force of a point charge and forms a Coulomb barrier when interacting with another proton at a distance $\approx Rq$ from the center. Such radiation of the electric field of the proton is currently taken as the basis for the formation of the Coulomb barrier and its effect on external charged particles (**Figure 11**).

However, in reality, the dynamics of the interaction of quarks in the proton leads to dynamical changes in the surface charge density of the proton:

$$\sigma_i \approx +e/4\pi R^2 \pm \Delta\sigma_i, \tag{25}$$

where: $\Delta\sigma_i$ is the maximum amplitude of the charge density change.

As a result of changes in the charge density on the proton surface, the external electric field pulsates in the radial direction: the field strength increases above the region of increasing charge density and decreases above the region of decreasing density (**Figure 13**).

In addition, the configuration of the electric field **E** is affected by the dynamics of proton motion in the atomic nucleus (**Figure 14**).

Changes in the surface charge density and masses of the proton, its rotation, and oscillations lead to multimode pulsations of the electric field strength ΔE , resulting in randomly occurring short-lived regions with different heights of the Coulomb barrier along the outer boundary of the nucleus, with the electric field oscillating with a maximum amplitude modulation coefficient of up to 30%. These fluctuations of the proton electric field strength lead to short-term radial jumps of the potential both in height and in minimum and, consequently, to deviations of the Coulomb barrier value from the average **U** value. The oscillating electric field of the proton around the nucleus is shown in (**Figure 15, 16**).

Summary of Proton Field Dynamics.

The electric field of the proton propagates radially, forming in space a region with an oscillating potential barrier: the amplitude modulation coefficient of the field strength is up to 30%, the relative change in the spatial potential $\Delta U/ U_{\max} = \Delta R/Rq = 0.5$, and the frequency of multimode oscillations of the field is in the ranges of nuclear transformations and dynamic displacements 10^{21} - 10^{23} Hz.

The changes in the magnitudes of the electric field of the proton, as compared to the field of a point charge, are explained by the following:

- Dynamically changing surface charge density $\sigma \approx +e/4\pi R^2 \pm \Delta\sigma$;
- Periodic changes in the proton mass density.
- The dynamics of proton motion within the atom.

(iii) Peculiarities of the Coulomb Field Formation by a Proton and a Neutron (Deuterium Atom Nucleus).

The magnitude and configuration of the electric field of the deuterium nucleus are determined by the electric properties of the proton and neutron, their mutual location, and their motion within the nucleus. The nuclear forces acting between nucleons are much larger than the Coulomb repulsion forces between protons. These forces arise only between a proton and a neutron in close proximity, with a limited range of action of approximately $\approx 10^{-15}$ m.

Characteristics of nuclear forces include:

- They are charge-independent, meaning they are non-electric in nature.
- They depend on the mutual orientation of the spins of the interacting proton and neutron.
- They are not central forces, meaning they do not act along the line connecting the centers of interacting nucleons.

The formation of the electric field strength and configuration of the nucleus is influenced by:

(a) Mechanical imbalance of the rotating masses of the proton and neutron in the nucleus.

The imbalance results in precession of the proton and neutron rotation axes, leading to relative vibrational and rotational motions between them. This dynamic movement introduces additional variations in the amplitude and frequency of the proton's electric field, contributing to pulsations in the Coulomb barrier potential. Consequently, short-lived regions with fluctuating Coulomb barrier heights appear along the outer boundary of the nucleus.

(b) Screening of the electric field by the neutron.

Neutrons have low electric field permeability, effectively acting as a local shield that weakens the proton's electric field in its shadow region by approximately a factor of **10** (corresponding to a reduction of about **-20 dB**). This screening effect results in the formation of a Coulomb field characterized by spatially divergent electric field rays, with a distinctive disruption along the axis of the neutron's location. As the nucleus moves, transient local regions of reduced potential emerge around it, contributing to fluctuations in the external electric field landscape.

The electric field of the deuterium nucleus is formed by oscillating radial beams with a localized region of low potential, influenced by factors (a) and (b). This electric field rotates with the nucleus along the x, y, and z axes, while also oscillating in amplitude and frequency. As a result, transient low-potential channels emerge within the Coulomb field volume of the nucleus, potentially allowing external microparticles to penetrate the nucleus (**Figure 17**).

(iv) Characteristics of the Coulomb Field Formed by a Proton and Two Neutrons (Tritium Nucleus).

The configuration of the electric field within the tritium nucleus is determined by the electric properties of its proton and two neutrons, their spatial arrangement, and their motion within the nucleus. Nuclear forces bind these nucleons, with the proton typically at the core and the neutrons either adjoining it or occupying a higher-level shell. This nucleon arrangement is synchronized by their respective fields, resulting in rotational and vibrational motion characteristic of an atomic nucleus.

The proton's electric field extends radially, partially shielded by the surrounding neutrons (**a**, **b**). Depending on the structural variant of the nucleus, the second-shell neutron may further shield the field (**c**) (**Figure 18**).

- Two neutrons are positioned on opposite sides of the outer level, aligned coaxially with the proton
- Two neutrons are placed at the outer level along the nucleus's radii. c. Both neutrons are situated on one side of the outer level, coaxial with the proton.

- In the oscillating Coulomb field of the nucleus, temporary low-potential channels emerge, potentially allowing external microparticles to enter the nucleus.
- The arrows indicate the direction toward the radial channel for potential microparticle entry (B denotes the entrance area of the local channel region).

Factors Influencing the Electric Field Formation:

(a) Mechanical Imbalance of the Rotating Proton and Neutrons: The imbalance causes precession of the rotational axes, resulting in simultaneous dipole and quadrupole oscillations. Additionally, nucleons exhibit random fluctuations due to their relatively weak binding in the outer shell. These fluctuations lead to shifts in the Coulomb barrier, creating a multimodal pulsation of the barrier potential. Consequently, transient regions with varying Coulomb barrier heights form along the nucleus's outer boundary.

(b) Shielding Effect of Neutrons: Neutrons act as localized dielectric shields, weakening the proton's electric field by approximately **20 dB** in shadow regions. This occurs due to the polarization of the neutron's internal structure, reducing the field strength. The shielding creates a non-uniform Coulomb field with spatial rays exhibiting one (**-20 dB**) or two (**-40 dB**) field dips. As a result, short-lived, rotating low-potential regions appear around the nucleus (**Figure 19**).

The electric field of the tritium nucleus radiates outward, oscillating with an amplitude modulation factor of up to **30%** within a frequency range of **10^{21} to 10^{23} Hz**. The two neutrons shield the proton's electric field, resulting in a divergent Coulomb field with spatial rays. Two local regions (a, b) exhibit a field strength drop of up to **-20 dB**, while a single region (c) shows a deeper dip of up to **-40 dB** relative to the average Coulomb field. These dynamic regions alter their angular positions, creating opportunities for low-energy external microparticles to enter the nucleus when aligned with the channel's cross-section (**Figure 19**).

Introduction to the Study Results

1. Formation of the Coulomb Barrier by Atomic Nuclei.

The Coulomb barrier of a nucleus is traditionally described as a continuous energy barrier characterized by a height **U** and width **a**, defined for a given energy by entry and exit points. The passage of low-potential microparticles, such as protons, is explained solely by quantum mechanical tunneling. Consequently, overcoming the barrier with positively charged particles possessing less than 100 times its energy has been addressed only through mathematical models, lacking a physical explanation. Our study demonstrates that the formation of the nuclear electric field follows these principles:

- The proton's electric field propagates radially, oscillating with an amplitude modulation factor of up to 30% within the frequency range of $10^{21} - 10^{23}$ Hz.
- Neutrons in the nucleus partially shield the proton's electric field, resulting in a Coulomb field composed of divergent spatial rays. This shielding leads to the emergence of local regions forming radial channels with reduced potential barriers.
- In these localized regions, the Coulomb barrier height U decreases by a factor of **10 to 100** or more compared to the average barrier potential for nuclei with a small number of protons and neutrons. Conversely, U increases as the atomic number rises. The entrance cross-sectional area of radial channels is approximately $S = \pi \cdot (1.2 \cdot R_n)^2$, where $R_n = 4.5616 \cdot 10^{-16}$ m, the neutron radius.
- These low-potential radial channels rotate with the nucleus, creating transient pathways through which low-energy microparticles can enter when aligned with the cross-sectional region (Figures 18 and 19).
- The Coulomb barrier height is defined as the electrostatic energy of interacting charged particles, accounting for the configuration of their electric fields as determined by amplitude directional diagrams (ADD):

$$U = \frac{1}{4\pi\epsilon_0} \cdot \frac{q_1 \cdot q_2}{R} \cdot F_1 \cdot F_2 \quad (26)$$

where: ϵ_0 - Permittivity of free space, q_1, q_2 - charges of interacting particles; R - interaction radius, $F_1(\theta_i, \phi_i, t_i)$ and $F_2(\theta_i, \phi_i, t_i)$ - Normalized ADDs of the electric fields of both interacting charges, as functions of angular coordinates and time.

For two interacting atomic nuclei outside the influence of nuclear forces, the Coulomb barrier is estimated using a simplified model:

$$U = 1,44 \cdot \frac{Z_1 \cdot Z_2}{R} \cdot F_1 \cdot F_2, \quad (27)$$

where: U - value of Coulomb barrier (MeV), $Z_1 = +e n_1, Z_2 = +e n_2$ - Charge numbers of nuclei **1** and **2**, Z - atomic number, R - distance between the nuclei in (f) ($1_f = 10^{-15}$ m.), with $R > r_0, r_0$ - radius of nuclear force interaction, $F_1(\theta_i, \phi_i, t_i)$ and $F_2(\theta_i, \phi_i, t_i)$ are the normalized ADDs of the electric fields of the two nuclei.

Normalized ADD ($F_i / F_{\max} \leq 1$) represents a three-dimensional surface illustrating the spatial distribution of a nucleus's Coulomb field at a fixed distance at a given time (**Figure 20**).

The height of the potential barrier U for two interacting nuclei depends on the magnitude of their charges, structural configuration, and spatial orientation at the moment of interaction. An estimation of the potential barrier U for four configurations of interacting charges is shown in **Figure 21**. A comparison of the U_{\max} potential barrier levels for different variants of interacting nuclei reveals the following:

- For two protons modeled as point charges with a static electric field, the maximum value of the potential barrier is approximately **1 MeV**.
- For two protons with oscillating electric fields, the Coulomb barrier decreases to about **500 keV**. If the protons' electric fields oscillate in phase, the barrier further decreases to around **250 keV**.

- When two deuterium nuclei approach each other along the axis of low-potential channels, the potential barrier is approximately **5 keV**.
- When two tritium nuclei with a linear structure (see Figure 21) approach each other, the potential barrier in the channel is about **50 eV**, which is roughly **10⁴ times** lower than the currently accepted barrier level for protons.

For a nuclear reaction to occur, atomic nuclei must have enough kinetic energy to overcome the Coulomb barrier **U_{max}**, reach the range of nuclear forces, and enter into interaction.

Using expression (27), we can determine the potential barrier **U_{max}** for interacting nuclei based on their spatial orientation. This allows us to estimate the probability of a charged particle penetrating the nucleus through a suprabar transition.

For instance, two tritium nuclei can approach each other to a distance of **10⁻¹⁵ m** within the range of nuclear forces if they converge through the radial channels with low potential. A kinetic energy of approximately **50 eV** is sufficient to overcome the Coulomb barrier under these conditions (**Option D**).

Thus, the existence of low-potential channels in the Coulomb field of nuclei enables particles to overcome the Coulomb barrier, whose average value is typically much higher than their energy. This phenomenon suggests that the overcoming of the Coulomb barrier by low-energy particles occurs in localized zones through the suprabar transition. It also offers a classical explanation for the tunneling effect.

2. Qualitative Estimation of the Probability of Charged Microparticles Passing Through the Coulomb Potential Barrier.

Microparticles must possess sufficient energy to surpass the height of the Coulomb barrier along their trajectory. While high-energy microparticles can overcome the barrier from any direction due to their kinetic energy, low-energy particles can only do so through localized regions with a certain probability. Our research suggests that the tunneling effect is a result of the presence of low-potential radial channels in the Coulomb field of nuclei. These channels provide a pathway through which charged particles can penetrate the Coulomb barrier, whose average value is significantly higher than their energy. The likelihood of a low-energy microparticle overcoming the barrier depends on the spatial orientation of the interacting particles, the width of the Coulomb barrier, and the kinetic energy of the nuclei.

Spatial orientation of interacting particles.

Charged microparticles, such as atomic nuclei, can enter the low-potential channels of the Coulomb barrier with a certain probability. The probability of microparticles passing through the barrier is determined by the angle and position of the axes of the radial channels of the interacting particles. This probability can be derived from geometric relations. For example, for two particles, where each has local regions with low-potential channels in its Coulomb field (i), and the case where only one particle has such a region (ii), the probability of such a coincidence depends on the ratio of areas:

$$\mathbf{P} = \mathbf{S}_{c1}/\mathbf{S}_{q1} \cdot \mathbf{S}_{c2}/\mathbf{S}_{q2} \quad (\text{i}) \quad (29)$$

$$\mathbf{P} = \mathbf{S}_{c1}/\mathbf{S}_{q1} \quad (\text{ii})$$

where: \mathbf{S}_{c1} and \mathbf{S}_{c2} are the areas of the entrance cross-section of the radial channels in the electric field of the two particles (with $\mathbf{S}_{c1} \approx \mathbf{S}_{c2} \approx \mathbf{S}_c = \pi \cdot (\mathbf{1}, \mathbf{1} \cdot \mathbf{R}_n)^2$, where $\mathbf{R}_n = 4.5616 \cdot 10^{-16} \text{ m}$ is the radius of the neutron), \mathbf{S}_{q1} and \mathbf{S}_{q2} are the areas of the spatial sphere of the Coulomb barrier ($\mathbf{S}_{q1} \approx \mathbf{S}_{q2} \approx \mathbf{S}_q = 4 \cdot \pi \cdot \mathbf{R}_g^2$, where \mathbf{R}_g is the radius of the spatial area of the Coulomb barrier, $\mathbf{R}_g \approx 4 \cdot \mathbf{R}_n$).

For example, for two interacting particles (i), the probability of axial convergence through low-potential channels is about **1/256**, and the probability of one particle entering the radial channel of the other (ii) is about **1/16**.

Width of the Coulomb Barrier and the Speed of Microparticles

The probability of an atomic nucleus overcoming the Coulomb barrier is greater when the barrier width is smaller and the kinetic energy is higher. This is explained by the dynamics of the motion of nuclei in space, which leads to changes in the electric fields with localized regions during the passage of microparticles through them. The time for changes in the spatial position of the radial channels in localized regions should be longer than the time it takes for a microparticle to pass through these channels:

$$\mathbf{T} > \mathbf{a} / \mathbf{V} \quad (30)$$

where: \mathbf{T} is the minimum time interval for a change in the spatial position of the nucleus's electric field ($\approx 10^{-20} \text{ sec}$), \mathbf{a} is the thickness of the potential barrier (approximately 10^{-15} m), \mathbf{V} is the average velocity of the nuclei in the radial channel of the Coulomb field, given by $\mathbf{V} = \sqrt{2 \cdot \mathbf{E}/\mathbf{m}}$.

From equation (30), it follows that the velocity of the nuclei for passing through the radial channel must be greater than $\mathbf{V} \geq 10^5 \text{ m/sec}$, which corresponds to the kinetic energy of low-energy protons $\mathbf{E} \geq 50 \text{ eV}$.

Probability of Microparticles Reaching the Nuclear Force Zone.

As a result of charge interactions, a proton must enter a region of approximately 10^{-15} m in size to be captured by the nuclear forces of the nucleus. In general, the probability of a reaction between two light nuclei approaching each other is proportional to $\approx \text{Exp} - (\mathbf{K} \cdot \mathbf{Z}_1 \cdot \mathbf{Z}_2 / \sqrt{\mathbf{W}})$, where: \mathbf{Z}_1 and \mathbf{Z}_2 are the numbers of protons in the interacting nuclei, \mathbf{W} is the energy of their relative proximity, and \mathbf{K} is a constant multiplier. The energy required for the reaction depends on the number of protons in each nucleus. If it is greater than three, this energy is too high and the reaction is practically unfeasible. Thus, as \mathbf{Z}_1 and \mathbf{Z}_2 increase, the probability of reaction decreases.

Well-known calculations show that the probability of nuclear interaction between particles is relatively low because of the small values of fusion reaction cross-sections, measured in barns (**1 barn** = 10^{-28} m^2). For example, the maximum fusion reaction cross-section for deuterium and tritium nuclei at energy of their relative proximity **100...200 keV**. is equal to about 5 barn ($5 \cdot 10^{-28} \text{ m}^2$), and at energy **20 keV** the cross section becomes less than **0.1 barn**. The distance between atoms is approximately $1.2 \cdot 10^{-10} \text{ m}$. at a temperature of **100 keV** ($\mathbf{T} = 1.16 \times 10^9 \text{ K}$) and the radius of the nuclear force zone is

10^{-15} m. This means that the distance between atoms is about 10^5 times larger than the area where protons must reach to pass the Coulomb barrier. Therefore, the probability of protons reaching the nuclear force zone should be small, on the order of 10^{-5} ... 10^{-6} . The calculation shows that out of about a million charged microparticles, no more than one pair should enter into nuclear interaction. The remaining particles dissipate their energy and slow down to speeds at which the reaction becomes impossible. However, in practice, this probability is much higher, as evidenced by the fusion process occurring on the Sun, where $T \approx 2 \cdot 10^6$ K and $P \approx 4.5 \cdot 10^8$ atm. Currently, there is no clear explanation for this phenomenon.

Our study shows that the higher probability of protons hitting atomic nuclei can be explained by the action of the Coulomb field of nuclei, which takes the form of divergent spatial rays with low electric field strength in localized regions. Around each nucleus, radial local regions with low potential arise, through which protons enter and continue to move radially toward the nucleus according to the principle of least resistance. In this way, the electric field of the nucleus, with its divergent beams, increases the effective cross-section of the fusion reaction by a factor of about **10 to 100**, enhancing the probability of protons hitting the nucleus by about **100 times**. This increases the probability of protons reaching the nuclear force zone to values on the order of 10^{-3} to 10^{-4} , which is consistent with practical observations.

Significance.

Scientific and Practical Importance.

Understanding the processes behind the tunneling effect is crucial both scientifically and practically. Currently, the well-known quantum mechanical explanation of the tunneling effect provides only a mathematical model and does not offer a true understanding of the underlying physical mechanism. The result of this work is a new explanation of the physical processes involved in the tunneling effect. It is established that the overcoming of the Coulomb barrier by low-energy microparticles occurs exclusively through a suprabarrier mechanism via a radial channel within the Coulomb barrier, characterized by a low potential level. The formation of these local regions in the Coulomb barrier, in the form of radial channels, is linked to the properties of atomic nuclei and their electric fields. This explanation is fully consistent with the results of nuclear physics and resolves the apparent contradiction between the tunneling effect and the laws of classical physics.

Expanded Understanding of the Tunnel Effect.

The findings of this work suggest that not only has the physical nature of the tunneling effect been clarified, but many parameters and characteristics of its manifestation have also been explained. These include the potential levels in the Coulomb barrier and its local regions for different nuclei, the oscillation parameters of elemental field strengths, and the probabilistic characteristics of microparticles passing through the barrier based on the spatial orientation of the nuclei.

A comparative evaluation confirms the accuracy of these results, aligning them with numerous experimental data and phenomena observed in the tunneling effect. In particular, the understanding of the physical processes behind the tunneling effect explains the increase in the transparency coefficient of the Coulomb barrier and the growth in the reaction cross-section when the spatial orientation of interacting atomic nuclei is controlled within the medium. These processes also account for the results

of several well-known experiments on low-temperature nuclear fusion and demonstrate the real possibility of nuclear fusion reactions, such as the fusion of two tritium nuclei at an average temperature of about 10^4 K. In particular, the physical processes of the tunnel effect make it possible to explain the well-known experiments on low-temperature nuclear fusion in the crystalline structures of titana (Ti) or polladium (Pb): the Fleischmann and Pons experiment on the study of the reaction of cold nuclear fusion (1989), the NASA Glenn Research Center experiment on "lattice confinement fusion" (2024), etc.

Practical Significance for Energy Solutions.

The new explanation of the physical processes of the tunneling effect carries significant practical implications, especially for solving energy-related challenges. A deeper understanding of this phenomenon opens up the potential to control the tunneling effect, enabling the creation of future energy systems and the production of unlimited energy resources.

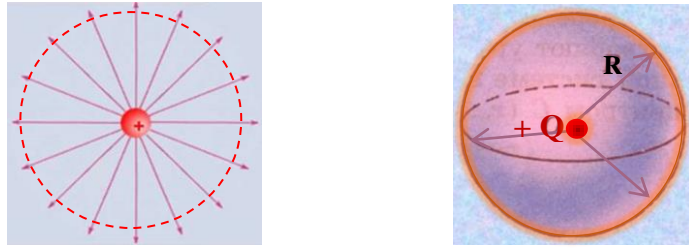


Figure 1. Electric field strength lines of point charge $+Q$ on the plane and in the volume in the form of spheres.

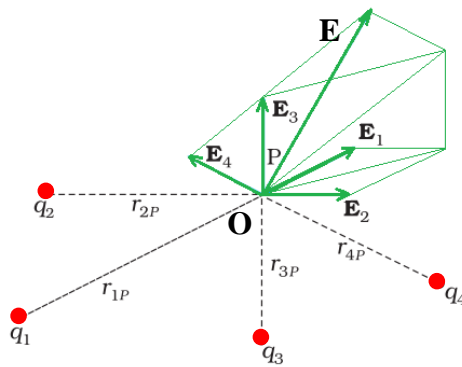


Figure 2. Electrostatic field of point charges q_1, \dots, q_4 is determined by the principle of superposition by adding vector values of the strengths of all charges (r_1, r_2, \dots, r_m) - position vectors relative to the center O , E_1, \dots, E_4 - field strengths of charges at the point P , E - resultant field strength).

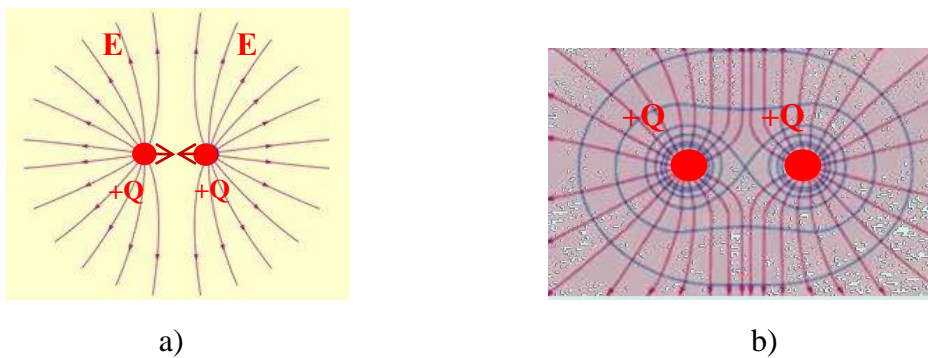


Figure 3. Electrostatic field strength E of two identical point charges $+Q$ (a) increases as they get closer together (b)

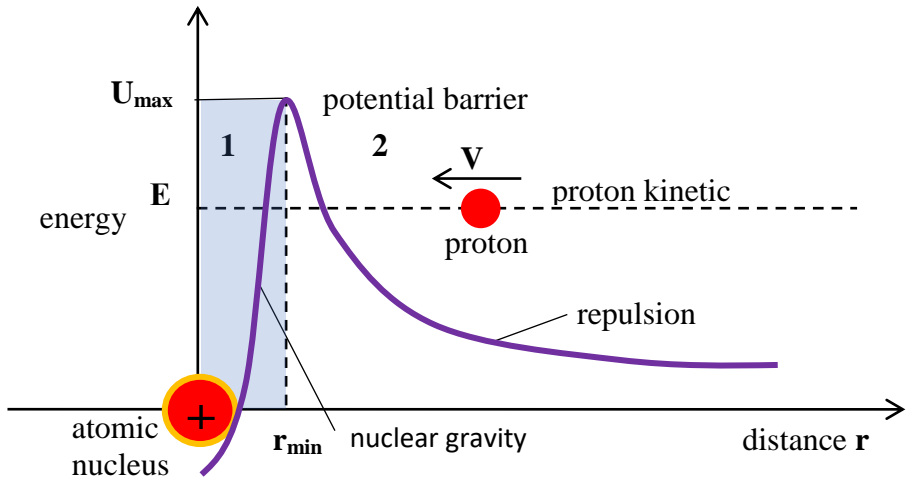


Figure 4. Approximate dependence of the total interaction potential of nuclei on distance has a maximum (the top of the Coulomb barrier) at some distance and the two regions of space 1 and 2 are separated by a potential barrier.

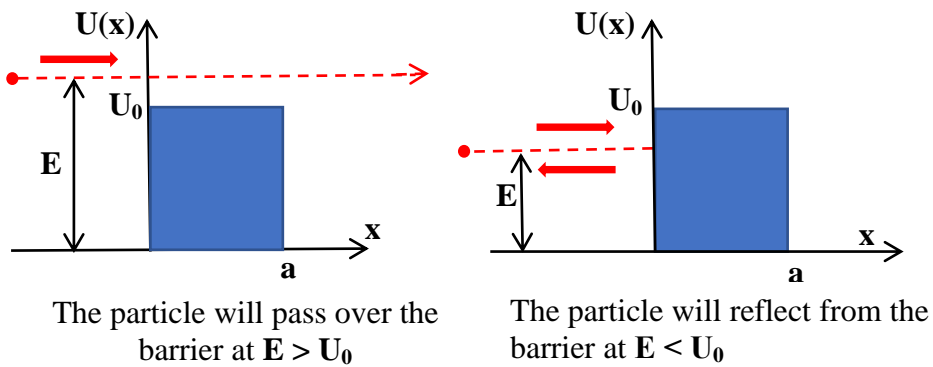


Figure 5. Potential Barrier in the Framework of Classical Mechanics

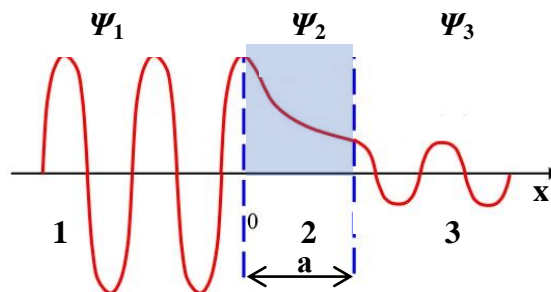


Figure 6. View of Ψ -functions (de Broglie waves) for different regions when microparticles pass through the potential barrier (ψ_1 - de Broglie wave with frequency f and amplitude A_1 , $\psi_2 \neq 0$, ψ_3 - de Broglie wave with frequency f and amplitude $A_3 < A_1$).

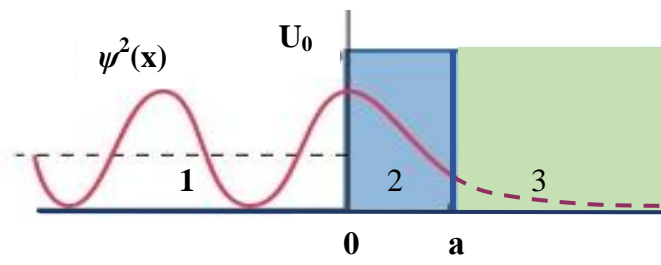


Figure 7. Collision of particles with potential barrier in quantum mechanics

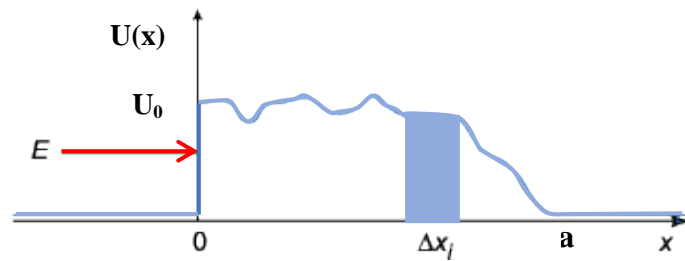


Figure 8. Potential barrier of arbitrary shape with thickness a

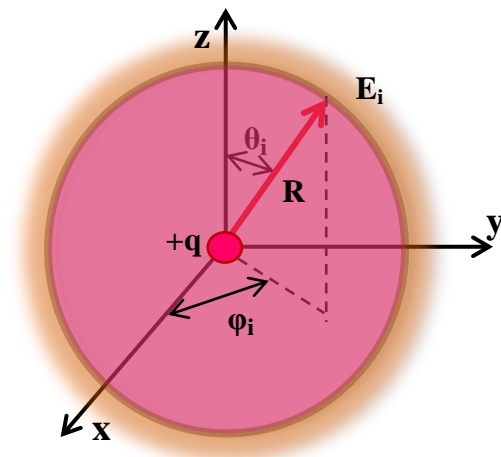


Figure 9. Amplitude diagram of the electric field directional (ADD) strength E of a point charge in the form of spheres at time $t = t_i$ (example).

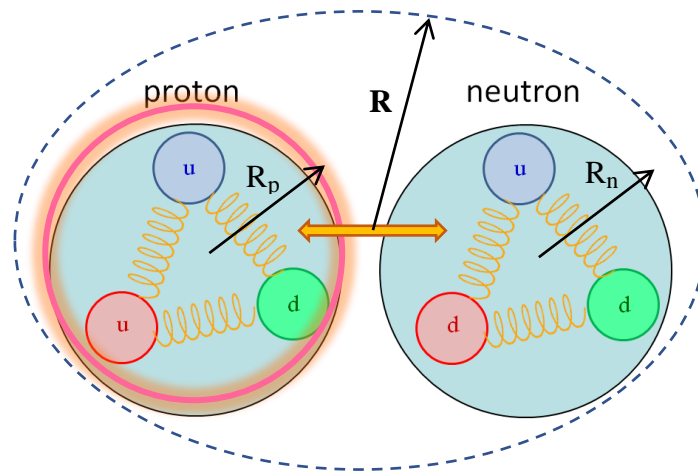


Figure 10. Structure of the nucleons (simplified version): proton consists of two up quarks U with charge $+2/3 e$ and one down quark d with charge $-1/3 e$, neutron consists of two down quarks d and one up quark U . The radius of the proton and neutron $R_{pn} \sim 4.5616 \cdot 10^{-16} m$.

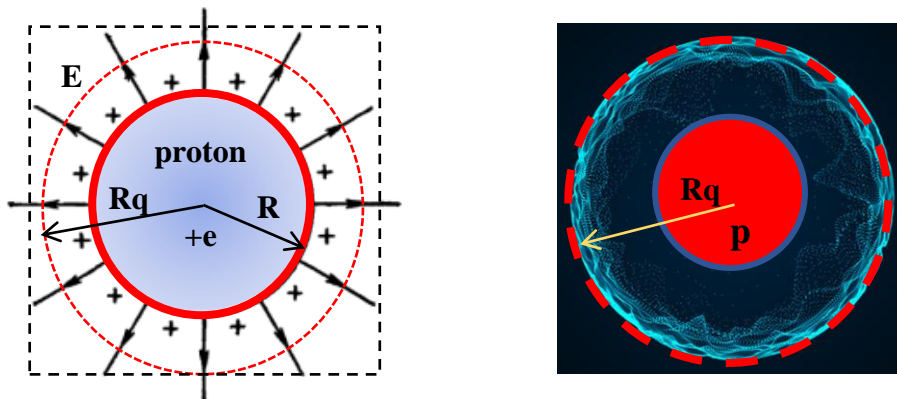


Figure 11. A Known Simplified Version of Proton Emission: the force lines of the electric field E of the proton are directed along the extension of the proton's radii and uniformly distributed like the force lines of a point charge (R is the radius of the proton, R_q is the radius of the spatial region of the Coulomb barrier when interacting with another proton).

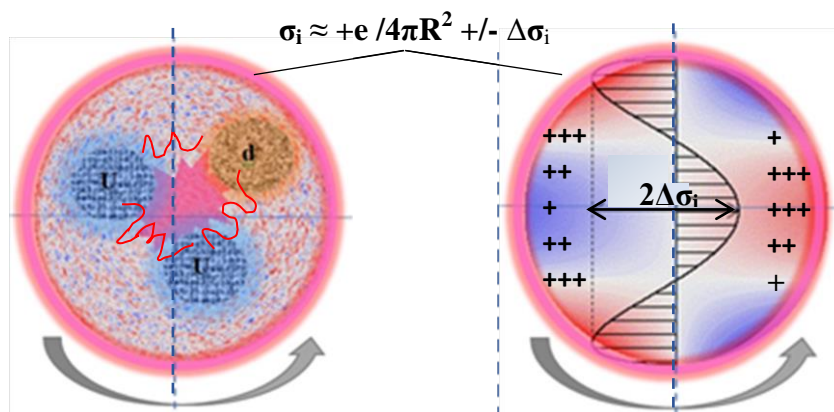


Figure 12. Interactions of Quarks U and d in the Proton Structure: these interactions lead to a periodic change in the charge density $\Delta\sigma_i$ on the proton surface and a change in the external electric field strength ΔE , respectively.

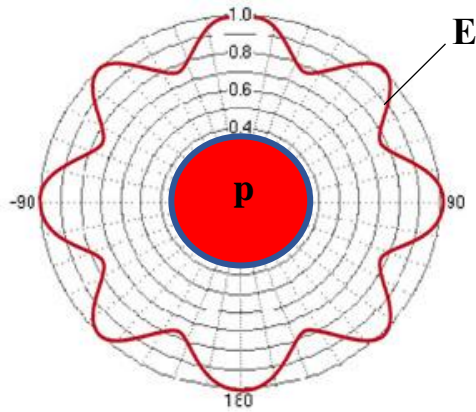


Figure 13. Cross Section of the Normalized ADN of the Proton's Bulk Electric Field: changes in the surface charge density of the proton lead to oscillation of its electric field.

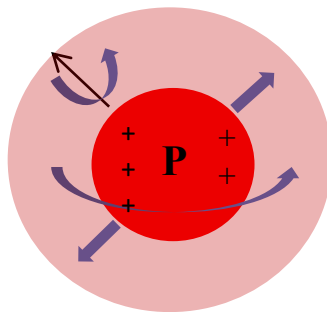


Figure 14. Oscillatory and Rotational Motions of the Proton in the Nucleus: these motions lead to additional fluctuations of the electric field E of the proton.

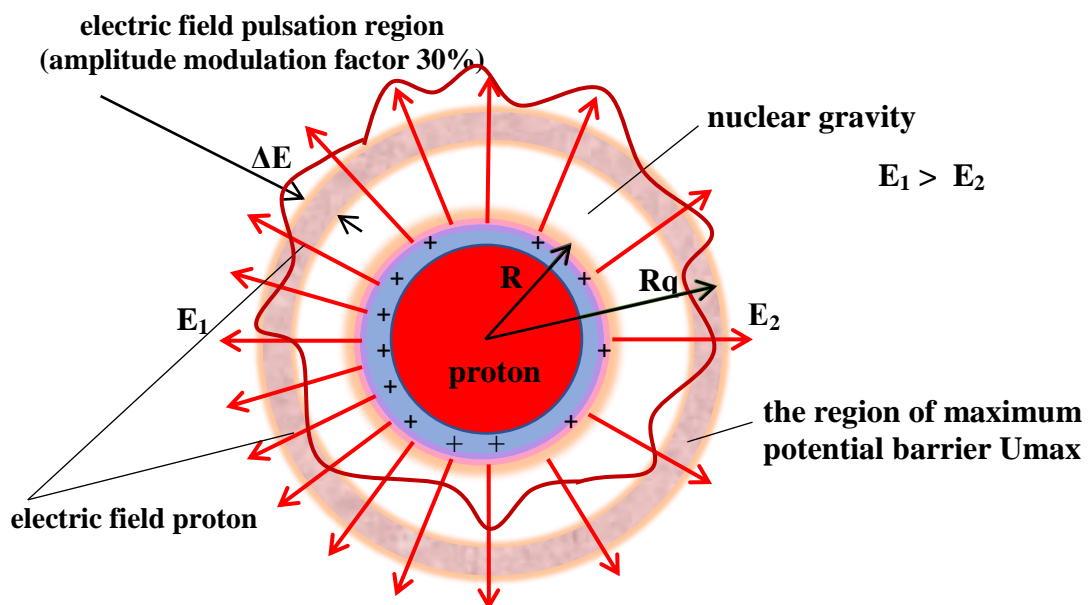


Figure 15. The Electric Field E of the Proton (Hydrogen Atom Nucleus): the field pulsates due to changes in surface charge and mass densities and proton motion.

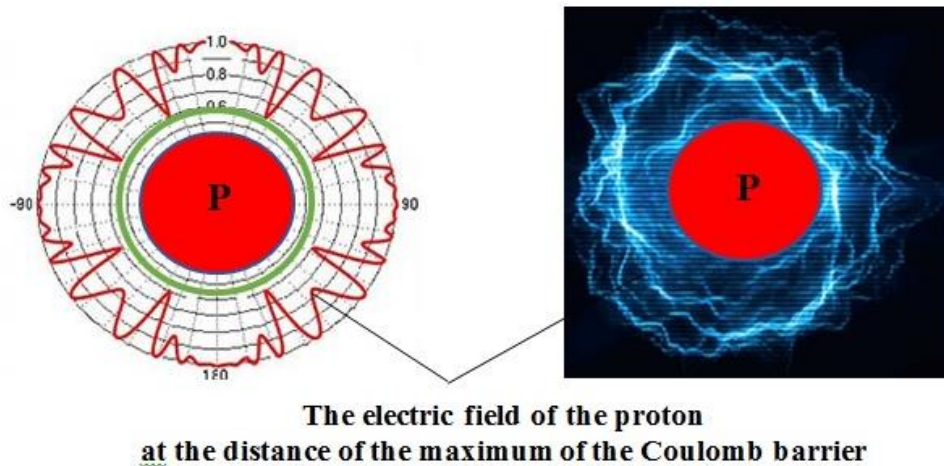


Figure 16. The Electric Field Along the Outer Boundary of the Proton Nucleus: this field is an oscillating multimode electric field.

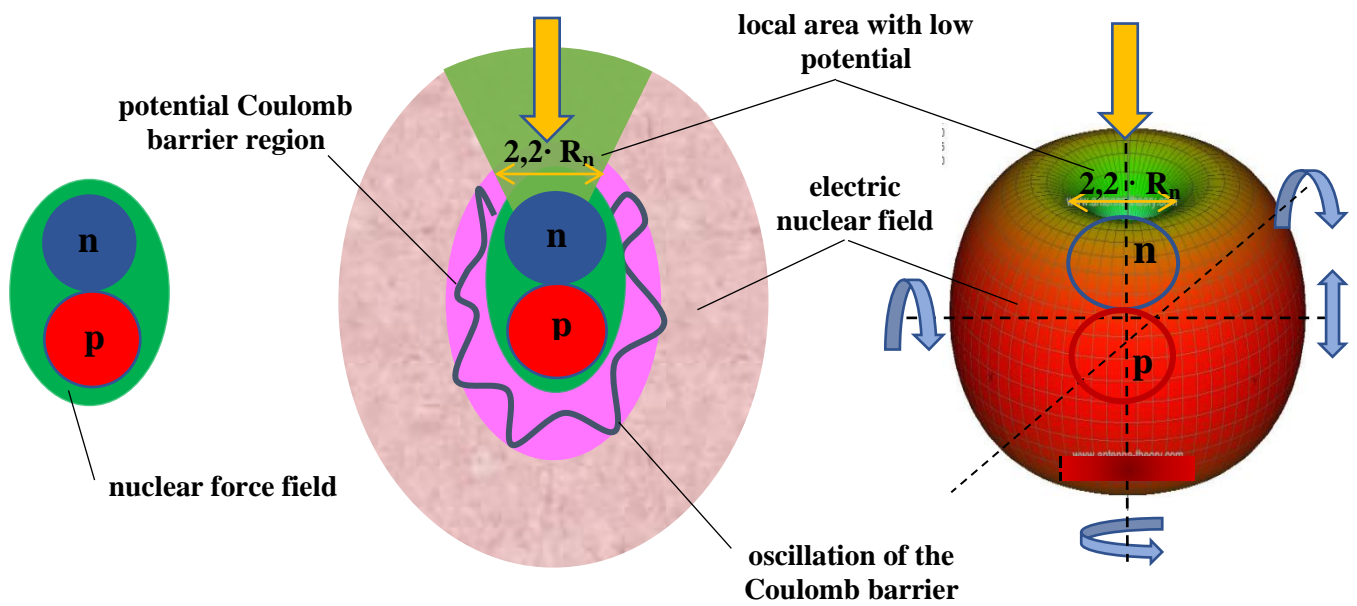


Figure 17. Oscillating Radial Beams of the Deuterium Nucleus: the nucleus's electric field rotates and oscillates in amplitude and frequency, forming transient low-potential channels that could allow external microparticles to penetrate the nucleus. $2.2 \cdot R_n$ is the diameter of the channel in the local region, where $R_n = 4.5616 \cdot 10^{-16} \text{ m}$, which is neutron's radius.

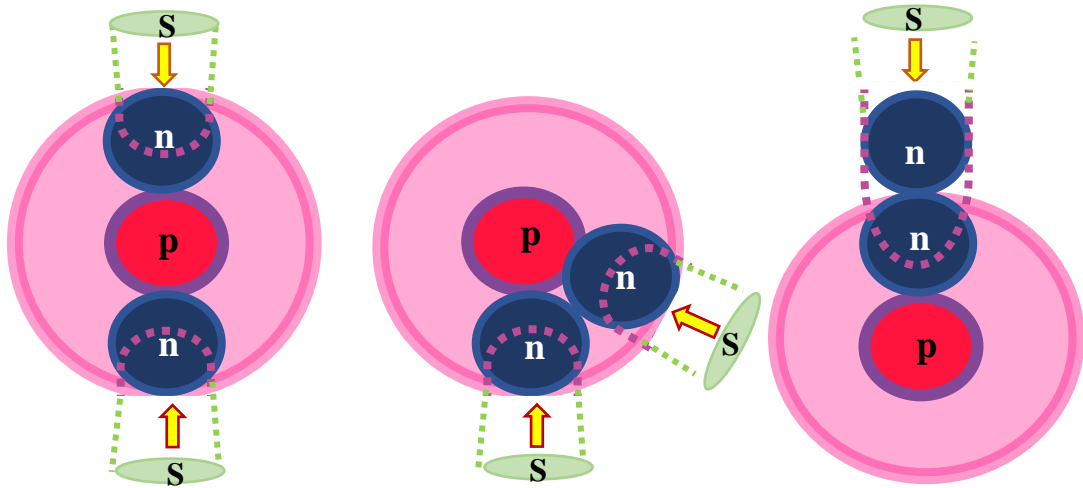


Figure 18. The structure of a tritium nucleus formed from a proton and two neutrons, which leads to the formation of spatial regions with low potential in the electric field of the proton.

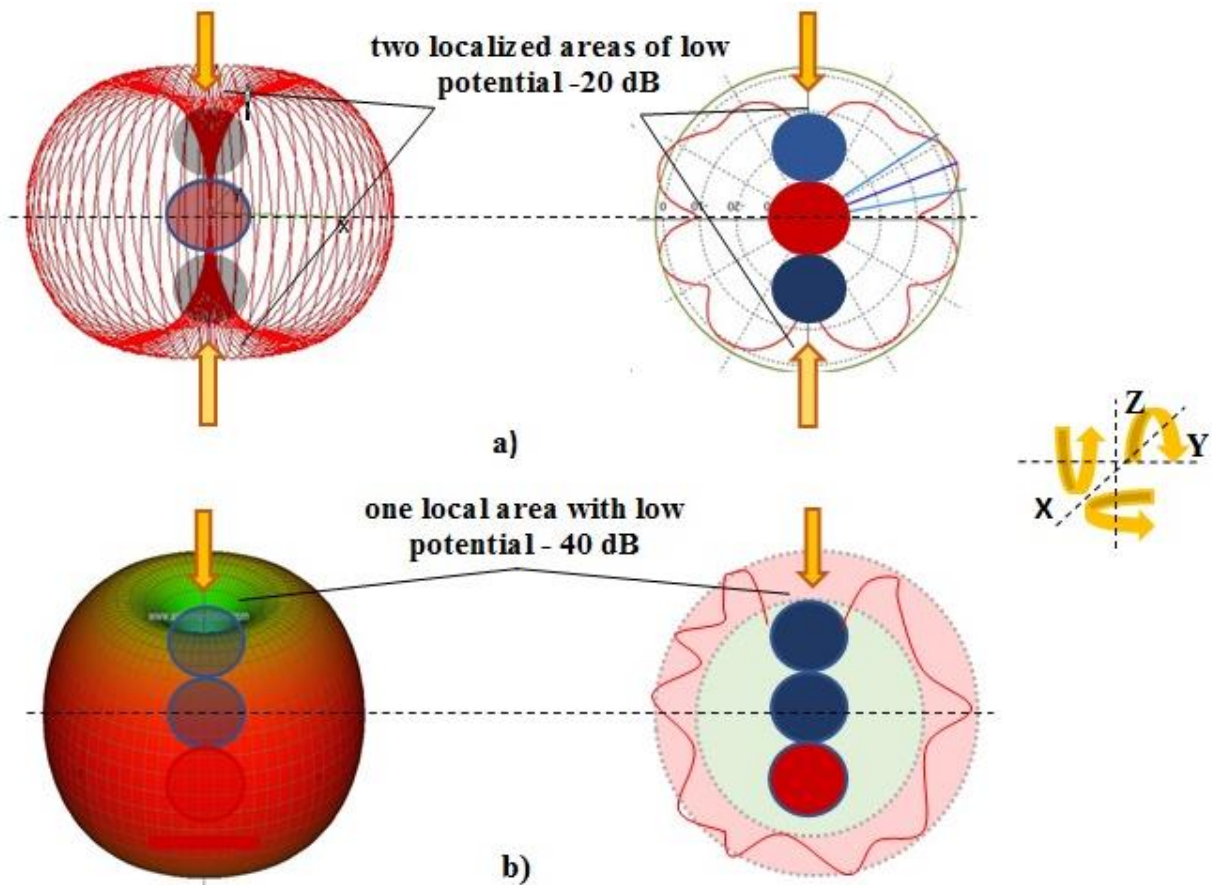


Figure 19. Low-potential channels are formed in the Coulomb field of the tritium nucleus and provide probable passage of microparticles into the nucleus:

(a) Two local areas of low potential (- 20 dB),

(b) One local area of low potential (- 40 dB).

*the arrows show the direction into a low-potential radial channel with the channel entrance cross-sectional area $S = \pi \cdot (1.1 \cdot Rn)^2$, where $Rn = 4.5616 \cdot 10^{-16}$ meters - neutron radius)

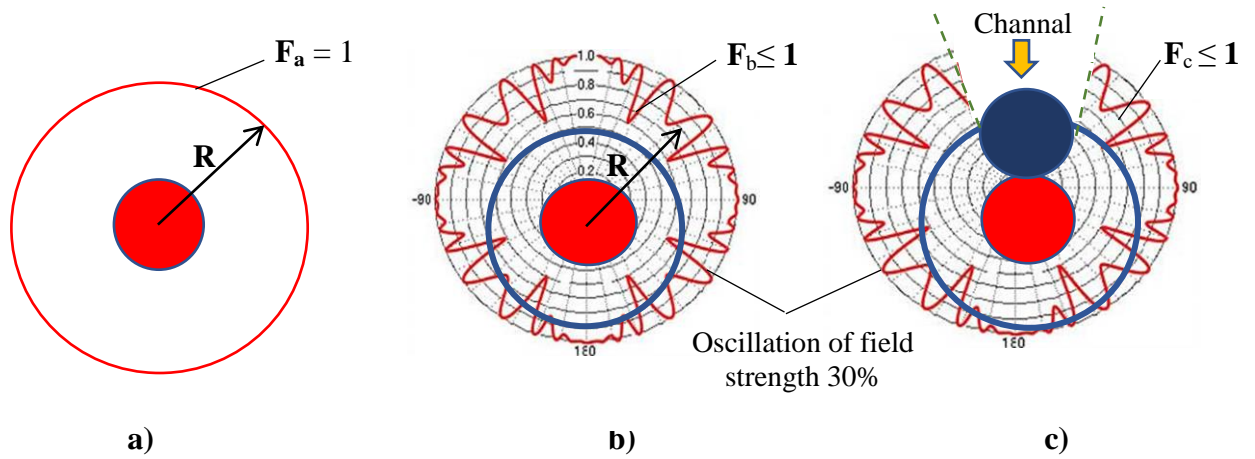


Figure 20. Cross section of the normalized Amplitude Directional Diagrams (ADDs) F_a , F_b , and F_c representing the electric fields of various nuclei at an equal distance R from their centers:
 F_a - Ideal electric field of a proton modeled as a point charge.
 F_b - Proton's electric field modeled as an oscillating, multimode field with a modulation factor of 30%.
 F_c - Deuterium's electric field depicted as an oscillating, multimode field with a 30% modulation factor, featuring a single low- potential channel (- 20 dB).
 R - the average radius of the spatial region corresponding to the Coulomb barrier.

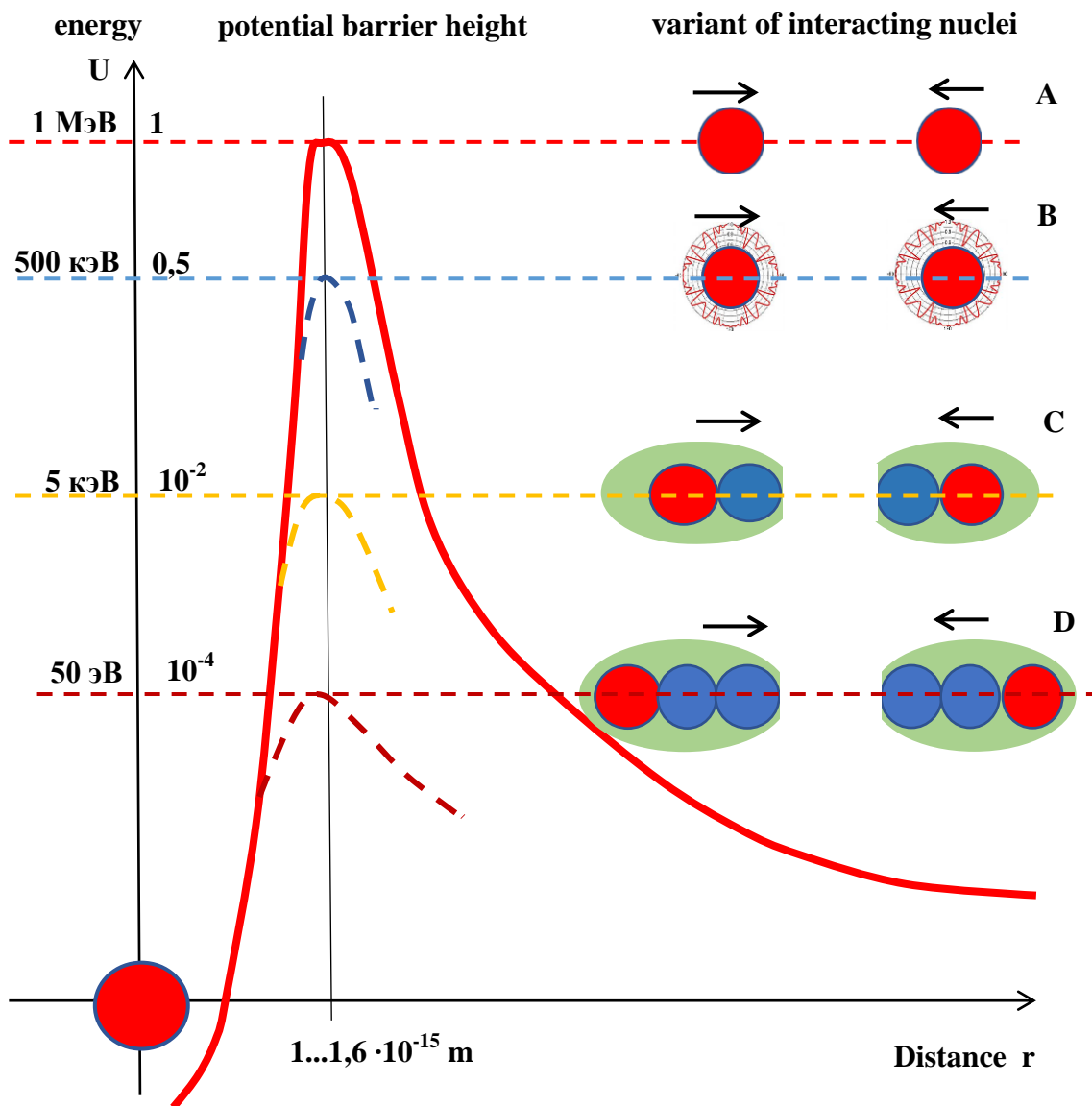


Figure 21 — The maximum potential barrier U_{\max} between interacting nuclei is influenced by their structural configuration and spatial orientation during approach:

A: Interaction of two protons modeled as point charges (ideal scenario).

B: Interaction of two protons with oscillating electric fields.

C: Interaction of two deuterium nuclei (proton + neutron) with opposing orientations of low-potential channels in their electric fields.

D: Interaction of two tritium nuclei (proton + two neutrons) with opposing orientations of low-potential channels in their electric fields.

References.

1. Tunnel effect // The Big Soviet Encyclopedia: [in 30 vol.] / ed. by A. M. Prokhorov. - 3rd ed. - M. : Soviet Encyclopedia, 1969-1978.
2. [https://ru.wikipedia.org/wiki/Tunnel effect](https://ru.wikipedia.org/wiki/Tunnel_effect).
3. Delaunay N.B. Tunnel effect. /Soros Educational Journal. № 1, 2000.
4. Razavy Mohsen. Quantum Theory of Tunneling. - 2nd. - Singapore: World Scientific Publishing Co., 2013. - 820 c. - ISBN 9814525006.
5. Kozhushner M.A. Tunnel phenomena.- M.: Znanie, 1983.-64 p.-Novoe v zhizn, nauka, tekhnika. Series: "Physics", No. 3).
6. Goldansky V. I. I., Trakhtenberg L. I., Flyorov V. N. Tunnel phenomena in chemical physics. Moscow: Nauka, 1986. - 296 c.
7. Bell, Ronald Percy (1980). "The tunnel effect in chemistry". London: Chapman and Hall. ISBN 0412213400. OCLC 6854792.
8. Purcell, Edward. Electricity and Magnetism, 2nd Ed. - Cambridge University Press, 2011. - P. 8-9. - ISBN 978-1139503556.
9. Richard Feynman. The Feynman Lectures on Physics Vol II. - Addison Wesley Longman, 1970. - P. 1-3, 1-4. - ISBN 978-0-201-02115-8.
10. Filonovich S. R. Coulomb's Law // Physical Encyclopedia : [in 5 vol.] / Ed. by A. M. Prokhorov. - Moscow: Soviet Encyclopedia, 1990. - T. 2:
11. Markushin V. E. Coulomb barrier of the nucleus // Physical Encyclopedia : [in 5 vol.] / Ed. by A. M. Prokhorov. - Moscow: Soviet Encyclopedia, 1990.
12. Razavy Mohsen. Quantum Theory of Tunneling. - 2nd. - Singapore: World Scientific Publishing Co., 2013. - 820 c. - ISBN 9814525006.
13. Wichmann E. Berkeley course of physics. Volume 4. Quantum physics. - Moscow: "Nauka", 1977 - 416 pp.
14. Razavi, Mohsen (2003). A quantum theory of tunneling. River Edge, New Jersey: World Scientific. ISBN 978-981-238-019-7. OCLC 52498470.
15. Kosarev A.V. Fundamentals of the Theory of Low Energy Nuclear Reactors. - M. Izd-e "Academy of Trinitarianism", 2023. - 223c. II
16. Some remarks about tunnel effect (review) G. Ivchenkov, Ph.D., kashey@kwic.com.
17. Lavrov A. S. Antenna-feeder devices: textbook for universities / A. S. Lavrov, G. B. Reznikov. - Moscow: "Soviet Radio", 1974. - 368 c.
18. Dudnik P. I. Multifunctional radar systems: textbook for higher educational institutions / P. I. Dudnik A. R. Ilchuk [and others]. - Moscow: Drofa, 2007. - 283 c. - ISBN 978-5-358-00196-1.
19. Beckman I.N. Nuclear Physics. Course of lectures. MOSCOW STATE UNIVERSITY. Moscow,
20. Shirokov Y.M., Yudin N.P. Nuclear physics. - Moscow: "Nauka", 1972. – 672 c.
21. Alexandrov Y.A. "Fundamental Properties of the Neutron". Moscow: Energoizdat, 1982.2
22. Barsukov O.A., "Fundamentals of Atomic Nucleus Physics. Nuclear Technologies." Moscow, Fizmatlit, 2011. 2